Electron localization in n-$Pb_{1-x}Eu_xTe$

A. Prinz, G. Brunthaler, Y. Ueta, G. Springholz, and G. Bauer
Institut für Halbleiterphysik, Universität Linz, A-4040 Linz, Austria

G. Grabecki and T. Dietl
Institute of Physics, Polish Academy of Sciences, al. Lotników 32/46, PL-02668 Warszawa, Poland
(Received 30 April 1998)

The electrical resistivity of Bi-doped $Pb_{1-x}Eu_xTe$ epitaxial layers with electron concentration $n \approx 2 \times 10^{17}$ cm^{-3} is studied as a function of temperature, magnetic field, and Eu content x. A metal-insulator transition is observed for x close to 0.1. It is found that the large static dielectric constant of this ionic material $\epsilon \approx 10^3$ modifies the electron localization compared to standard doped semiconductor systems in two ways. First, the localization is not driven by ionized impurity potentials but rather by short-range alloy scattering, which is particularly efficient due to large offsets between the conduction bands of PbTe and EuTe. Second, only the singlet particle-hole channel of the disorder-modified electron-electron interaction is presumably contributing to electron localization. This leads to the absence of the corresponding magnetoconductance, and reduces the destructive effect of electron-electron scattering on phase coherence. As a result, negative magnetoresistance brought about by interference of self-crossing trajectories is observed up to temperatures as high as 100 K. [S0163-1829(99)09019-0]

I. INTRODUCTION

It has been known for a long time that effects of electron correlations as well as potential fluctuations associated with the Coulomb impurity potentials play a crucial role in carrier localization in doped semiconductors.[1] In particular, disorder-modified electron-electron interactions give rise to quantum corrections to the Boltzmann conductivity, which drive presumably the metal-insulator transition (MIT).[1–3] The Hubbard on-site repulsion, in turn, is thought to account for the presence of localized moments already on the metallic side of the MIT.[1,4] Finally, electron-electron scattering appears to be the main phase breaking mechanism at low temperatures.[3,5]

Here, we present results of magnetoconductance studies as a function of Eu content in ternary Bi-doped $Pb_{1-x}Eu_xTe$ layers grown by molecular beam epitaxy (MBE). A drastic decrease of the low-temperature electron mobility is observed with increasing Eu content x. The mobility drops from about 1×10^6 cm^2/Vs for PbTe to 1000 cm^2/Vs in the case of $Pb_{0.92}Eu_{0.08}Te$ for an electron concentration of 2×10^{17} cm^{-3}. For these values, the product of the Fermi wave vector k_F times the mean-free-path of the electrons l approaches one. This indicates the possibility for a disorder-induced MIT, even in the absence of the magnetic field, in stark contrast to n-PbTe, in which the onset of electron localization has appeared in a 20 T field range.[6] The MIT is indeed found for $Pb_{1-x}Eu_xTe$ with x about 0.1, as evidenced by temperature-dependent conductivity measurements. The magnetoresistance of the studied samples shows a positive and a negative component. The former is weakly temperature dependent and scales with the mobility, suggesting that it originates from an effect of the Lorentz force and the associated Landau quantization. The latter is well described based on the concepts by Kawabata[7] and Altshuler and co-workers,[3,8] and its analysis provides the magnitude and temperature dependence of the phase coherence length.

An analysis of the accumulated findings shows that the specific feature of this material system is its large static dielectric constant $\epsilon \approx 10^3$ resulting from the fact that PbTe is at the borderline to a ferroelectric phase transition due to a cubic-rhombohedral distortion.[9] In particular, localization appears *not* to be driven by ionized impurity potentials but rather by short-range alloy scattering, which is particularly efficient due to large offsets between the relevant bands of PbTe and EuTe. Furthermore, only the singlet particle-hole channel of the disorder-modified electron-electron interactions is presumably operating, as its magnitude does not depend on the electron charge.[3] This leads to the absence of the magnetoconductance driven by the interactions, and reduces their destructive effect on the phase coherence. Owing to a small magnitude of the sp-f exchange coupling at the L-point of the Brillouin zone,[10,11] also the spins localized on the $4f$ shell of Eu ions have virtually no influence on the electron phase. As a result, negative magnetoresistance brought about by interference of self-crossing trajectories is observed in a wide temperature range up to 100 K. The negative magnetoresistance in the studied range of Eu concentrations is, therefore, of a different origin than that in EuTe,[12,13] where a destructive effect of the magnetic field on bound magnetic polarons plays a dominant role.

Our paper is organized as follows. In Sec. II, the growth procedure and sample characterization is presented. Experimental results and their interpretation are summarized in Sec. III, where the issues of alloy and spin-dependent scattering, metal-insulator transition, and magnetoresistance are described. Section IV contains the main conclusions of the paper. In Appendix A, details about the dependence of the effective mass on the Eu content are given.

II. GROWTH AND CHARACTERIZATION OF $Pb_{1-x}Eu_xTe$:Bi EPILAYERS

A. Growth procedure

N-type $Pb_{1-x}Eu_xTe$ epilayers with Eu contents between $x=0$ and 0.3 and a thickness of 3 μm were deposited on

freshly cleaved BaF_2 (111) substrates in a Riber 1000 MBE system equipped with standard effusion cells for PbTe, Te, Eu, and Bi_2Te_3. Prior to the growth of the proper structures, the PbTe and Eu fluxes were calibrated by a quartz crystal microbalance moved to the substrate position. The substrates were preheated in two steps: first at 440 °C for 15 min in the preparation chamber, and then at 580 °C for 30 min in the main chamber. The $Pb_{1-x}Eu_xTe$ samples were grown at a growth rate of 1.1 μm/h and a Te/Eu beam flux ratio of 2. The substrate temperature was kept at 340 °C and continuous azimuthal rotation during growth ensured a high lateral homogeneity of both the Eu composition and the layer thickness. The element Bi supplied under chalcogen rich conditions has proven to be most efficient as *n*-type dopant. Occupying a substitutional metal-lattice site, the doping action is readily understood from the fact that the donor Bi has one electron more as compared to Pb. To facilitate complete incorporation of Bi, it is supplied in chalcogenide form as Bi_2Te_3, and doping levels as high as 10^{20} cm^{-3} have been achieved with a unity doping efficiency.[14,15] From a beam flux calibration of the Bi_2Te_3 effusion cell it was found that a cell temperature of 300 °C leads to the desired electron concentration $n=2\times10^{17}$ cm^{-3}.[16] The growth was monitored by *in situ* reflectivity of high energy electron diffraction (RHEED) employing a 35 keV beam at an incidence angle of 0.3°. The RHEED patterns demonstrate that $Pb_{1-x}Eu_xTe$ nucleates in the form of three-dimensional (3D) islands on the substrate, and as the growth proceeds, the islands start to coalesce and merge together to form a smooth 2D surface after about 500-nm layer deposition. This scenario has been confirmed by visualization of the surface structure as a function of the epilayer thickness by means of scanning tunneling microscopy.[17]

B. Sample characterization

After deposition, the samples were characterized by high-resolution x-ray diffraction in both Ω and $\Omega/2\theta$ directions. Open detector and triple axis modes were used for scans of the [222] Bragg reflection. The full width at half maximum (FWHM) of the rocking curves increases from about 30 arcsec for $x=0$ to 150 arcsec for $x=0.2$. Additionally, the values of Eu content x as given by the flux calibration were compared, and found to agree in the range considered here $x\leqslant0.15$, with the results of chemical analysis using atomic emission spectroscopy. In several samples with different Eu concentration, the magnetic susceptibility was investigated. It was found that the paramagnetic Curie temperature is strictly proportional to the x content up to $x=0.30$.[18] This effect originates from separated Eu ions, as in contrary, nearest Eu neighbors show antiferromagnetic behavior. These findings demonstrate that the Eu ions are incorporated substitutionally and no considerable clustering occurs in the PbEuTe layers.

In IV-VI compounds, the minima of the conduction band are at the L points of the Brillouin zone, so that there are four equivalent valleys oriented along the $\langle111\rangle$ directions. We expect, however, that because of the difference between thermal expansion coefficients of BaF_2 and $Pb_{1-x}Eu_xTe$, the epilayers will be under tensile stress at low temperatures. As a result, the fourfold degeneracy of the L states is lifted and, for the growth direction parallel to the $\langle111\rangle$ direction, the valley with its main axis oriented along $\langle111\rangle$ is shifted downwards in energy as compared to the three obliquely oriented valleys. The magnitude of the valley splitting depends on the actual values of strain and deformation-potential tensor, and is of the order of 5 meV for PbTe on BaF_2 at 4.2 K.[19,20] Of course, for Fermi energies smaller than this splitting, just one valley is occupied. At given electron concentration, the tendency toward occupation of one valley should increase with the Eu content as, according to data presented in Appendix A, the effective masses increases, and hence E_F decreases, with x.

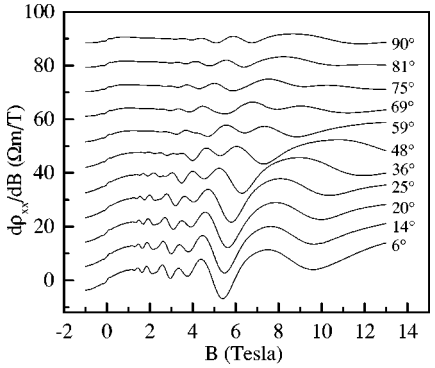

FIG. 1. First derivative of the resistivity with respect to the magnetic field for $Pb_{1-x}Eu_xTe$ sample with $x=0.04$. The oscillations are caused by the Shubnikov–de Haas effect; θ denotes the angle between the magnetic field and the $\langle111\rangle$-direction perpendicular to the layer.

In order to determine the occupation of the different conduction band valleys, measurements of the Shubnikov–de Haas (SdH) effect were performed in the magnetic field up to 14 T and at the temperature of 0.3 K. As shown in Fig. 1, the magnetoresistance oscillations are well resolved in $Pb_{1-x}Eu_xTe$ with $x=0.04$. By contrast, in the case of samples with higher Eu content, the scattering damping precluded the meaningful examination of the effect.

The spectrum of the SdH magnetoresistance oscillations is known to be determined by the fundamental frequencies B_i and its higher harmonics,[21,22] where B_i are proportional to the cross sections of the Fermi surface in the direction perpendicular to the magnetic field,

$$B_i=2\pi E_F^{(i)}m_c^{(i)}/\hbar e. \tag{1}$$

Here $E_F^{(i)}$ and $m_c^{(i)}$ are the Fermi energy and the cyclotron mass in ith valley.

Our SdH measurements were performed at different angles θ between the magnetic field and the $\langle111\rangle$ direction where the field was rotated into the current direction along $\langle01\bar{1}\rangle$. Figure 1 shows the first derivative of the measured resistivity with respect to the magnetic field B. By taking the first derivative, the background magnetoresistance is effectively suppressed and the accuracy of the period determination improved. The Fourier transform of the oscillations versus the inverse magnetic field for $\theta=6°$ is shown in the inset to Fig. 2. Two main maxima are seen to dominate the Fourier spectrum. The dependence of their positions on the angle θ is depicted in the main part of Fig. 2. In order to establish the origin of these two peaks, we calculated the angular depen-

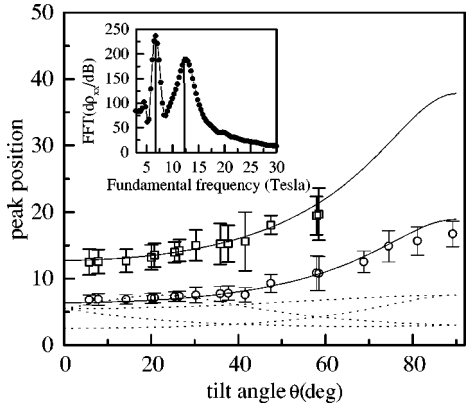

FIG. 2. Peak positions of the Fourier transform of $\partial\rho/\partial B$ for different tilt angles θ (open symbols, error bars represent the half width of the peaks). Full lines show the calculated fundamental frequency and its first harmonic (lower and upper solid line, respectively) assuming that only the $\langle 111\rangle$ valley is occupied. Dashed lines are calculated angular dependencies of the fundamental frequencies for the case of four equally occupied valleys. The inset shows the Fourier transform for $\theta = 6°$.

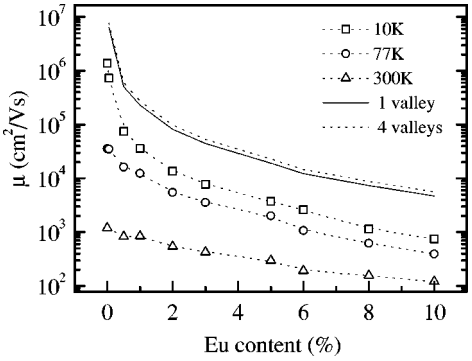

FIG. 3. Electron mobility for a set of $Pb_{1-x}Eu_xTe$ samples with Eu content $0 \leqslant x \leqslant 0.30$. The experimental points (marked by symbols) were determined at temperatures of 10, 77, and 300 K, the solid and dotted lines represent calculated values of mobility limited by alloy scattering in the case of one and four occupied valleys, respectively.

dence of the fundamental frequencies B_i assuming that either one valley or four valleys are occupied. By adapting the electron concentration $n_{SdH} = 2.7\times10^{17}$ cm^2, close to that determined by the low field Hall effect $n_H = 3.2\times10^{17}$ cm^2, we obtain a good description of the data under assumption that one valley is occupied and that the two maxima of the Fourier spectra correspond to the fundamental frequency B_1 and its first harmonics $2B_1$, respectively (solid lines in Fig. 2). At the same time, a similar magnitude of the two maxima is consistent with the fact that the spin-splitting is about two times smaller than the cyclotron energy in n-$Pb_{1-x}Eu_xTe$. By contrast, no agreement can be reached redistributing the electrons between the four valleys (dashed lines in Fig. 2). We conclude that the overwhelming majority of the carriers, about 85%, occupies the valley that is oriented along the $\langle 111\rangle$ direction. This is in agreement with the estimated values of strain and deformation potentials for PbTe on BaF_2.[19,20]

Electron concentration n and mobility μ were obtained from Hall effect and resistivity measurements in Van-der-Pauw geometry in the temperature range from room temperature down to 10 K. The parameters of the samples selected for magnetoresistance studies down to 1.5 or 0.3 K are summarized in Table I. A spherical and one-valley approximation has been adapted in order to evaluate the magnitude of the product of the Fermi wave vector k_F and mean-free-path l. It is seen that incorporation of Eu drives the system towards a strongly localized regime $k_F l < 1$.

III. EXPERIMENTAL RESULTS AND DISCUSSION

A. Alloy scattering

With increasing Eu content the energy gap of $Pb_{1-x}Eu_xTe$ enlarges drastically ($dE_g/dx = 4480$ meV at $T = 1.8$ K) for x below about 8%, above which a change to a smaller slope is observed.[23] This kink marks the appearance of an indirect gap,[23] associated presumably with a shift of the valence band top away from the L-point of the Brillouin zone.

Figure 3 presents electron mobilities at 10, 77, and 300 K, which decrease with increasing temperature and Eu content x. The latter is partly induced by an increase of the effective mass caused by a change of the energy gap. At room temperature, the mobility is limited by phonon scattering. The drop of mobility with x is, however, stronger at low temperatures,[24] which suggests the appearance of an additional scattering mechanism with the incorporation of Eu. The large magnitude of dE_g/dx points to a large efficiency of electron scattering by fluctuations of the conduction-band edge arising from a random distribution of the alloy constituents. For an uncorrelated cation distribution and neglecting

TABLE I. Electron concentrations and mobilities as well as the values of the mean free path and its product by the Fermi wave vector for the studied samples with Eu content between 0 and 0.15.

Sample	x_{Eu} (%)	n (cm^{-3})	μ (cm^2/Vs)	l (cm)	$k_F l$
595	0	1.00×10^{17}	957000	4.16×10^{-4}	597
447	1	3.59×10^{17}	36000	3.27×10^{-5}	45.3
450	4	3.20×10^{17}	6470	4.36×10^{-6}	9.23
400	6	1.60×10^{17}	1294	7.01×10^{-7}	1.18
453	8	2.10×10^{17}	1191	7.13×10^{-7}	1.31
695	9.5	1.10×10^{17}	538	2.61×10^{-7}	0.39
693	12.5	1.13×10^{17}	96	4.73×10^{-8}	0.07
455	15	1.20×10^{17}	50	2.51×10^{-8}	0.04

nonparabolicity of the conduction band, mobility $\mu_{\rm al}$ limited by alloy scattering is in the first Born approximation given by

$$\frac{1}{\mu_{\rm al}}=\frac{m_c^* m_d^*}{\pi\hbar^4 e}\sqrt{2m_d^*\varepsilon_F}\,\frac{V^2}{N_o}x(1-x). \tag{2}$$

Here, m_c^* and m_d^* are the conductivity and density-of-states effective masses, respectively; ε_F is the Fermi energy; N_o is the cation concentration, and the energy $V=dE_c/dx=bdE_g/dx$, where $b=0.55\pm0.2$ in the case of $Pb_{1-x}Eu_xTe$,[25] describes that part of the change of the energy gap E_g with x, which results from the shift of the conduction band edge.

The dependence of mobility limited by alloy scattering upon Eu content, calculated under the assumption that the electrons are equally distributed between the valleys or—because of thermal strain—occupied only one valley, are shown in Fig. 3 by the dotted and solid lines, respectively. The dependence of the effective mass on Eu content is taken from Geist *et al.*[11] for $x\leqslant 0.04$ and linearly extrapolated to larger x, as described in the Appendix. We see that the calculated mobility reproduces correctly the rapid decrease of the measured values with x. Such an unusual importance of alloy scattering stems from a strong influence of Eu-derived states upon the PbTe conduction band as well as from the virtual absence of competing scattering by ionized impurities, as the Coulomb part of their potentials is efficiently screened by the induced ionic polarization. It is seen also, however, that the theoretical values of the mobility are higher than the experimental ones, even for large x, where alloy scattering should dominate. As it will be explained in the subsection devoted to electron-electron interactions, we assign this disagreement to a large magnitude of corrections to the first Born approximation in IV-VI semiconductors at the localization boundary $k_F l\approx 1$.

B. Spin-dependent scattering

The magnetic character of Eu ions raises the question about the importance of spin-disorder scattering in the case of either electron mobility or phase coherence. Detailed studies[11] of electron spin-splitting by means of four wave-mixing have demonstrated that, in agreement with theoretical predictions,[10] the exchange coupling of the electrons and Eu spins is extremely weak in $Pb_{1-x}Eu_xTe$. For the appropriate values of the exchange energies, $B=5$ meV and $b_1\approx 0$, spin-disorder relaxation time for $n=2\times10^{17}$ cm^{-3} is longer than 10 ns, even for $x=0.1$.

Also spin-dependent scattering resulting from spin-orbit couplings appears to be of minor importance in the studied samples. In particular, because of inversion symmetry in the rock salt lattice, there is no crystal electric field which, in the case of zinc-blend structure, constitutes a source of efficient spin-dependent scattering, known as Dyakonov-Perel mechanism.[26] By contrast, the Elliot-Yafet mechanism,[26] which results from the mixing of the spin parts of the wave function by the combined effect of $k\cdot p$ and spin-orbit coupling could be effective in the narrow-gap semiconductors under consideration.[27] In a spherical approximation, the ratio of spin-dependent to spin-independent scattering rates in the case of alloy scattering reads

$$\frac{\tau_{\rm al}}{\tau_{\rm so}}=\frac{2}{3}\left(\frac{\varepsilon_F}{E_g}\right)^2\left(\frac{W}{V}\right)^2, \tag{3}$$

where $W=dE_v/dx=(1-b)dE_g/dx$ the shift of the *valence* band top with Eu content. For the parameters corresponding to $n=2\times10^{17}$ cm^{-3} and $x=0.05$ the above formula gives 5.1×10^{-4} or 8.1×10^{-5} depending on whether the carriers reside in one or in four valleys.

C. Electron-electron interaction

Altshuler and Aronov[28,3] have shown that disorder in electronic systems leads to profound modifications of the Fermi-liquid model. These modifications can be described by two diffusive modes, i.e., the particle-particle or Cooper channel and the particle-hole or diffuson channel. The Cooper channel, which corresponds to a spin-singlet state, enhances the conductivity σ and is as sensitive to the magnetic field as the weak localization correction. The particle-hole channel consists of a spin-singlet term, which results in a decrease of σ, and spin-triplet terms $(S_z=0,\pm1)$, which cause an increase of σ. The spin-triplet particle-hole channel is only sensitive to sufficiently large magnetic fields, such that the field-induced spin splitting becomes comparable to k_BT.

It might appear that the large dielectric constant of $Pb_{1-x}Eu_xTe$ will make effects of electron-electron interactions totally unimportant, at least in the temperature range $k_BT\leqslant\omega_{TO}$. Indeed, in the low-temperature limit, a typical energy transfer during processes of electron-electron scattering is smaller than the energy of the transverse optic phonons, so that the dynamic screening of the Coulomb interaction potential by lattice polarizability is rather efficient.[29] It has however been demonstrated by Schmid[30] and Altshuler and Aronov[3] that the diffusive character of the electron motion enhances—and makes dominant at low temperatures—a contribution from scattering involving a small momentum transfer. For such processes, the electron-electron interaction in the singlet particle-hole channel is determined by the Fourier transform of the screened Coulomb potential in the low-frequency and the small wave vector limits.[3] Under these circumstances, the effective potential does not depend on the value of the dielectric constant. Hence, the effects of the electron-electron interaction in the singlet particle-hole channel are expected to be present even in materials with an abnormally large dielectric constant such as $Pb_{1-x}Eu_xTe$. By contrast, the effective potentials in the remaining channels are much reduced by the lattice dielectric constant, as they are determined by the Fourier components averaged over the Fermi sphere.

The above considerations lead to a number of important conclusions. First, in standard materials the quantum corrections to the conductivity brought about by the one-electron localization and the interaction in the singlet particle-hole channel are known to be partly compensated by the antilocalizing contributions originating from the triplet particle-hole and the singlet particle-particle channels.[1–3] Since the latter terms are strongly reduced by the lattice polarizability in $Pb_{1-x}Eu_xTe$, we may expect that on approaching $k_Fl=1$,

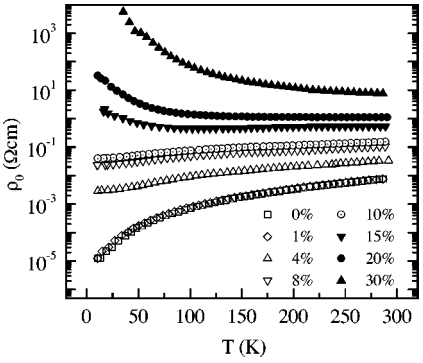

FIG. 4. Temperature dependence of resistivity for a set of $Pb_{1-x}Eu_xTe$ samples with Eu content x between 0 and 0.30. Open and full symbols represent metallic and insulating behavior, respectively.

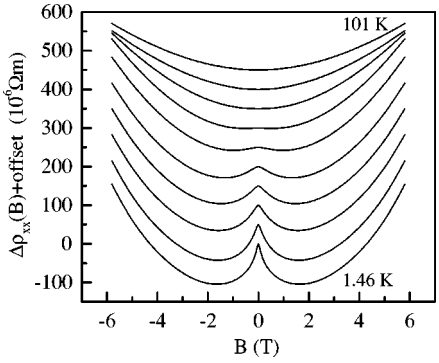

FIG. 6. Magnetoresistivity of $Pb_{1-x}Eu_xTe$ sample with $x=0.1$ at temperatures of 1.46, 4.26, 10.2, 15.1, 20.3, 30.3, 39.6, 60.1, 80.5, and 101 K. Except for the lowest temperature data, the curves are shifted upwards by incremental offsets of 50×10^{-6} Ω m at $B=0$ for clarity.

the conductance values will unusually strongly deviate from those predicted based on the first Born approximation. Most probably, this effect is responsible, at least partly, for the difference between the calculated and measured mobilities depicted in Fig. 3. Second, no magnetoconductance induced by the disorder-modified electron-electron interactions will be present, as it is associated with the interactions in those channels, which are reduced by the lattice screening. Finally, for the same reason the latter terms will not contribute to dephasing associated with electron-electron scattering. Accordingly, the phase-coherence length l_φ in $Pb_{1-x}Eu_xTe$ is expected to be limited only by the interaction in the singlet particle-hole channel and by the second inelastic-scattering process, the electron-phonon interaction. As the electron-electron scattering in the triplet channel is strongly suppressed in $Pb_{1-x}Eu_xTe$ the phase coherence length will be *larger* than in the case of, for instance, groups IV or III-V semiconductors.

D. Metal-to-insulator transition

The temperature dependence of the resistivity for a set of samples with the Eu content as a parameter is presented in Fig. 4. For one sample, containing 9.5% of Eu, the measurements were extended down to 0.1 K. As shown in Fig. 5,

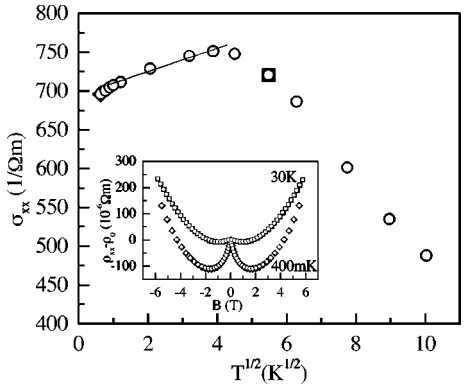

FIG. 5. Conductivity of $Pb_{1-x}Eu_xTe$ sample with $x=0.1$ versus square root of temperature. Localization effects are seen as a decrease of conductivity below 16 K (i.e., $T^{1/2}=4$ $K^{1/2}$). The inset shows magnetoresistivity at 0.4 and 30 K, whose negative component originates from coherent single-electron backscattering.

localization effects make the conductivity of this sample to decrease below 4 K, according to $\sigma=\sigma_o+mT^\alpha$, where $m>0$, and $\alpha\approx0.5$.

The data summarized in Figs. 4 and 5 demonstrate clearly the occurrence of a metal-to-insulator transition (MIT) around $x_c=10\%$ for which k_Fl is about 0.4. At this stage we are, however, unable to determine critical exponents that characterize the transition, since most data are outside the critical region where $(x-x_c)/x_c\ll1$. According to the analysis presented above, alloy scattering limits electron mobility. Consequently, we are led to the conclusion that the MIT is totally driven by scattering, not by electron localization on individual Coulomb impurities. Such MIT is caused by quantum effects brought about by one-electron localization and the singlet particle-hole term.[1] Due to the large dielectric constant in $Pb_{1-x}Eu_xTe$, the resulting quantum corrections to the conductivity are not compensated by the antilocalizing triplet particle-hole and singlet particle-particle contributions, as explained in the previous subsection. By the same reason, the MIT in question should not be perturbed by the formation of the local magnetic moments on the metal side of the MIT.[1]

E. Magnetoresistance

The magnetoresistance measurements performed on the $Pb_{1-x}Eu_xTe$ samples reveal the presence of both positive and negative contributions. The positive component is weakly temperature dependent and its magnitude increases with electron mobility. This magnetoresistance was analyzed in detail previously for the case of PbTe,[6] and results from the field-induced redistribution of the electrons between the Landau levels corresponding to different valleys as well as, above 5 T, from the onset of the field-induced localization.

The magnitude of the negative magnetoresistance increases on lowering temperature and on approaching the MIT. This indicates that it is associated with a localization effect. We interpret it as originating from a destructive influence of the magnetic field upon interference of self-crossing trajectories. In Fig. 6 experimental data for $x=9.5\%$ are shown for the temperature range from 1.46 to 101 K. Up to 40 K the one-electron localization effect is observed, as can be inferred from the presence of negative magnetoresistance.

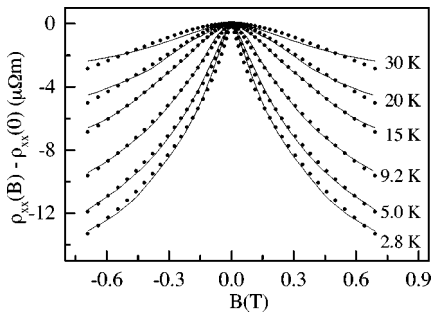

FIG. 7. Magnetoresistivity of $Pb_{1-x}Eu_xTe$ sample with $x=0.06$ at various temperature (points) compared to theoretical values (solid lines) calculated according to theory of coherent backscattering.

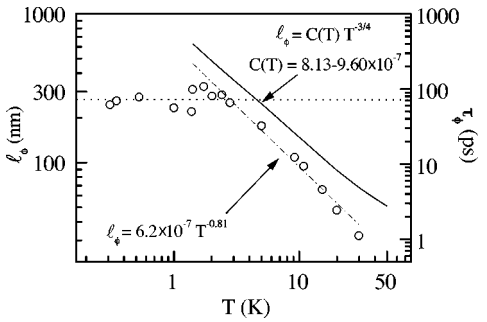

FIG. 8. Temperature dependence of the phase coherence length (or phase coherence time—right-hand scale) for $Pb_{1-x}Eu_xTe$ sample with $x=0.06$ at temperatures between 0.3 and 10 K. Solid line is calculated assuming that phase coherence is limited by electron-electron scattering in the electron-hole singlet channel.

In the sample with $x=15\%$, the negative magnetoresistance was even observed up to 100 K. The persistence of interference up to such high temperatures implies a rather long phase coherence length l_φ in comparison to the elastic mean-free-path l. This is consistent with a partial reduction of electron-electron scattering by lattice screening, as explained in Sec. III C.

It is worth noting also that for the same reason, despite a large magnitude electron spin-splitting and $k_F l \approx 1$, we do not observe positive magnetoresistance, which could be assigned to the effect of the electron-electron interactions.

The theoretical models that we adapted to analyze the negative magnetoresistance were developed by Kawabata[7] and Altshuler *et al.*[8,3] for anisotropic surfaces of constant energies and $k_F l \gg 1$. The correction to the diagonal magnetoconductivity tensor depends on $l_\varphi = (D_c \tau_\varphi)^{1/2}$, with D_c the ''cyclotron'' diffusion coefficient,[3] on the magnetic length $l_H = (\hbar/eH)^{1/2}$, and on the function f_3 (whose integral representation is given by Altshuler *et al.*[3]) appropriate for the 3D case for weak localization:

$$\delta\sigma_{ii} = \frac{e^2}{2\pi^2\hbar}\,\frac{f_{an}}{l_H}\,f_3\left(\frac{4l_\varphi^2}{l_H^2}\right). \tag{4}$$

In the above equation, the anisotropy factor $f_{an}=1$ in the case of one valley transport and a spherical Fermi surface as well as in the case of many valley systems provided that intervalley scattering time τ_v is shorter than τ_φ. In general, f_{an} depends on τ_v/τ_φ, the diffusion tensor, and the orientation of the magnetic field. We know from the analysis of the Shubnikov–de Haas oscillations that mainly the valley with the main axis along $\langle 111\rangle$ parallel to the growth direction is occupied. The contribution of the $\langle 111\rangle$ valley can be calculated from the general expression for the coherent backscattering of an isoenergetic surface of ellipsoidal shape[3] and leads to $f_{an} = (m_\parallel/m_\perp)^{1/2}$ and $l_\varphi = (D_\perp \tau_\varphi)^{1/2}$ with $D_\perp$ the diffusion constant along the effective mass $m_\perp$. In the case that the other three (oblique) valleys contribute to the conductivity corrections one has to add a second term of the form of Eq. (4) with $f_{an} = (h_2 m_\parallel/m_\perp)^{1/2} h_3$, $l_\varphi = (h_2 D_\perp \tau_\varphi)^{1/2}$, $h_2 = 1/3(1+8m_\perp/m_\parallel)^{1/2}$, and $h_3 = 1/3(5+4m_\perp/m_\parallel)$. Since the accurate values of the valley occupations and of the intervalley scattering rates are not well known, we shall treat f_{an} as a fitting parameter.

We compare the above theoretical prediction to experimental data obtained for the sample with 6% of Eu, which has the lowest Eu content where the negative magnetoresistance is not overcompensated by the positive contribution. The result of such a fit for temperatures up to 30 K and in the magnetic field up to 0.7 T is shown in Fig. 7, where experimental and theoretical values of the magnetoconductance $\sigma_{xx}(B)$ are depicted. In addition to f_{an}, a prefactor a of the positive magnetoresistance $\Delta\rho = aB^2$ and l_φ constitute the adjustable parameters. The parameter l_φ is assumed to be temperature dependent.

This procedure leads to $f_{an}=0.82$ and $a=2\times10^{-6}$ (Ω cm/T^2) as well as to $l_\varphi(T)$ presented in Fig. 8. Possible reasons for a prefactor smaller than one could be either a fast intervalley scattering process or the presence of a gradient in the conductance along the growth axis. We see that $l_\varphi(T)$ tends to saturate below 2 K. This saturation may result from the onset of spin-dependent scattering or it originates from phase breaking caused by external sources of high-frequency electromagnetic radiation.[31] The observed temperature dependence above 2 K, $l_\varphi(T) \sim T^{-0.81\pm0.1}$ suggests, in turn, that the screened electron-electron interactions starts to contribute, as for this phase-breaking mechanism Altshuler *et al.*[3,5] predict a $T^{-3/4}$ behavior.

Setting the screening factor F to zero in Eq. (4.4) of Altshuler *et al.*[3] and performing a temperature average over the quasiparticle energy as well as assuming that the relevant diffusion constant is the cyclotron diffusion constant D_c, one obtains $l_{\varphi,e\text{-}e} = C(T)T^{-3/4}$, with $C(T)$ varying from 8.13 to 9.60×10^{-7}, shown by a solid line in Fig. 8. The values of $l_{\varphi,e\text{-}e}$ obtained in this way are seen to be higher by about 50% than the experimental ones. This discrepancy may suggest some quantitative inaccuracies of the model or the presence of a contribution from another phase-breaking mechanism, such as electron-phonon scattering.

If we assume that the experimentally deduced phase coherence length l_φ consists of the two contributions from electron-electron ($l_{\varphi,e\text{-}e}$) and electron-phonon ($l_{\varphi,e\text{-}ph}$) interaction, we can estimate the size of the latter one by taking the difference of the respective phase-breaking scattering rates. We get $l_{\varphi,e\text{-}ph} \approx 9.36\times10^{-7}T^{-0.86}$ or $\tau_{\varphi,e\text{-}ph} \propto T^{-1.72}$. The dependence of the inelastic electron-phonon scattering time was investigated by Mittal *et al.*[32] in $GaAs/Al_xGa_{1-x}As$ two-dimensional electron gas samples. They found that this

time decreased due to disorder in the system. In the clean-limit ($k_F l \gg 1$) a dependence of the phase coherence time $\tau_\varphi \propto T^{-3}$ is expected.[33,34] For the dirty limit ($k_F l < 1$), the theoretically expected behavior is still controversial: a scattering time proportional to T^{-4} has been predicted by Thouless,[35] by Rammer and Schmid,[36] and by Reizer and Sergeyev,[37] whereas the calculations by Takayama[38] and by Kagan and Zhernov[39] and by Belitz and Das Sarma[40] give a T^{-2} behavior. It is, therefore, possible that we have a contribution to the phase relaxation time $\tau_\varphi(T)$ from electron-phonon interaction in the range above 3 K, though the experimentally determined magnitude of $\tau_{\varphi,e\text{-}ph}(T)$ has to be treated with caution as it is affected by uncertainties in the model of the electron-electron contribution.

IV. CONCLUSIONS

The experimental results and discussion presented above demonstrate that the peculiar features of electron localization in $Pb_{1-x}Eu_xTe$ stem from its large static dielectric constant, $\epsilon \approx 10^3$. In particular, in contrast to standard semiconductors, the metal-to-insulator transition appears to be driven by short-range alloy scattering, not by ionized impurity potentials. Furthermore, only the singlet particle-hole channel of the disorder-modified electron-electron interactions is operating, as its magnitude does not depend on the dielectric constant of the medium. This leads to the absence of the magnetoconductance driven by the interactions, and reduces their destructive effect on phase coherence. As a result, negative magnetoresistance brought about by interference of self-crossing trajectories is observed in a wide temperature range up to 100 K. The quantitative description of the data shows that the order of magnitude of both the negative magnetoresistance and the phase coherence length is correctly reproduced by current theory. It is at present unclear, however, whether a more accurate description of the data would require an extension of the theoretical model or rather more elaborated treatment of strain and multivalley effects in this material system.

ACKNOWLEDGMENTS

We thank M. Sawicki for experimental support with the SdH investigations. We thank FWF Vienna, ''Österreichische Nationalbank'' Project No. 6333, Ost-West Fonds, and GME in Austria, as well as KBN (Grant No. 2-P03B-6411) in Poland, for financial support. The work of Y.U. in Austria was supported by CNPq-Brazil (Proc. Nr. 260020/93-1).

APPENDIX: ELECTRON MASSES IN $Pb_{1-x}Eu_xTe$

The interband matrix elements $2P_\perp^2/m_0$ and $2P_\parallel^2/m_0$ for $Pb_{1-x}Eu_xTe$ with $x \leqslant 0.046$ were determined by Geist *et al.*[11] from magneto-optical investigations. The effective masses along ($m_\parallel$) and perpendicular ($m_\perp$) to the main axis of the ellipsoidal mass tensors at the L-points of the Brillouin zone can be calculated from the interband matrix elements by

$$\frac{1}{m_{\parallel,\perp}} = \frac{2P_{\parallel,\perp}^2}{m_0}\frac{m_0}{E_g(x)} + \frac{1}{m_{\parallel,\perp}^-}. \tag{A1}$$

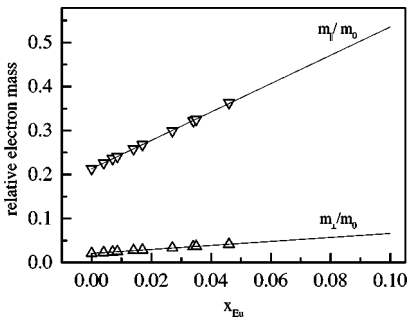

FIG. 9. Linear approximation to the dependence of the effective masses $m_\perp$ and $m_\parallel$ on the Eu content x in $Pb_{1-x}Eu_xTe$.

The far band contributions are $m_\parallel^- = 0.505 m_0$ and $m_\perp^- = 0.06 m_0$ for PbTe.[27] In order to calculate the effective masses for different x values, the dependence of the energy gap on the Eu concentration is needed. It is given at $T = 4.2$ K by[11]

$$E_g(\text{meV}) = 189.7 + 4480x. \tag{A2}$$

The perpendicular interband matrix element depends—within the accuracy of the experimental data points—linearly on x, whereas the parallel one is much better described by a polynom of second order.[11] By least-square fits we obtain $2P_\perp^2/m_0 = 6.02 - 65.93x$ and $2P_\parallel^2/m_0 = 0.51 - 1.76x - 60.49x^2$. Using a polynom of higher degree for extrapolation may result in arbitrary large deviations. Especially the expression for the parallel interband matrix element approaches zero and would—according to the above expression—become negative for $x > 0.078$, which is not allowed. We therefore calculated with the help of Eq. (A1) the effective masses and found that they depend—to a good approximation—linearly on the Eu content x. A linear least-square fit with fixed values at $x = 0$ gives

$$\frac{m_\parallel}{m_o} = 0.213 + 3.23x,$$

$$\frac{m_\perp}{m_o} = 0.0207 + 0.453x. \tag{A3}$$

The linear approximation is shown in Fig. 9 together with the values for the effective masses, which are calculated from the interband matrix elements given by Geist *et al.*[11] It was reported that around $x = 0.1$, the band gap changes from a direct one to an indirect one as Eu related bands enter the band gap from the valence band. In this region a different behavior of the interband matrix elements and the effective masses is expected.

We used the extrapolated masses according to Eq. (A3) up to an Eu content of 10%. The mass anisotropy ratio K is defined by

$$K = \frac{m_\parallel}{m_\perp}, \tag{A4}$$

and decreases from about 10.3 for PbTe to about 8.1 at $x = 0.1$.

[1] See D. Belitz and T. R. Kirkpatrick, Rev. Mod. Phys. **66**, 261 (1994).
[2] A. M. Finkelstein, Zh. Éksp. Teor. Fiz. **86**, 367 (1984) [Sov. Phys. JETP **59**, 212 (1984)]; C. Castellani, C. Di Castro, P. A. Lee, and M. Ma, Phys. Rev. B **30**, 527 (1984).
[3] See B. L. Altshuler and A. G. Aronov, in *Electron-Electron Interactions in Disordered Systems*, edited by A. L. Efros and M. Pollak (North-Holland, Amsterdam, 1985), p. 1; also, H. Fukuyama, *ibid*, p. 155; P. A. Lee and T. V. Ramakrishnan, Rev. Mod. Phys. **57**, 287 (1985).
[4] R. N. Bhatt, M. A. Paalanen, and S. Sachdev, J. Phys. (Paris) **49**, 1179 (1988).
[5] B. L. Altshuler, A. G. Aronov, and D. E. Khmel'nitskii, J. Phys. C **15**, 7367 (1982).
[6] J. Oswald, B. B. Goldberg, G. Bauer, and P. J. Stiles, Phys. Rev. B **40**, 3032 (1989).
[7] A. Kawabata, Solid State Commun. **34**, 431 (1980); J. Phys. Soc. Jpn. **49**, 6228 (1980).
[8] B. L. Altshuler, A. G. Aronov, A. I. Larkin, and D. E. Khmel'nitskii, Zh. Éksp. Teor. Fiz. **81**, 768 (1981) [Sov. Phys. JETP **54**, 411 (1981)].
[9] See, e.g., G. Bauer, W. Jantsch, and E. Bangert, in *Advances in Solid State Physics* edited by P. Grosse (Vieweg, Wiesbaden, 1983), Vol. XXIII, p. 27.
[10] T. Dietl, C. Śliwa, G. Bauer, and H. Pascher, Phys. Rev. B **49**, 2230 (1994).
[11] F. Geist, W. Herbst, C. Mejia-Garcia, H. Pascher, R. Rupprecht, Y. Ueta, G. Springholz, G. Bauer, and M. Tacke, Phys. Rev. B **56**, 13 042 (1997).
[12] Y. Shapira, S. Foner, N. F. Oliveira, Jr., and T. B. Reed, Phys. Rev. B **5**, 2634 (1972).
[13] J. Stankiewicz, S. von Molnar, and F. Holtzberg, J. Magn. Magn. Mater. **54-57**, 1217 (1986).
[14] D. L. Smith and V. Y. Pickardt, J. Electrochem. Soc. **125**, 2042 (1978).
[15] D. L. Partin, J. Electron. Mater. **10**, 313 (1981).
[16] A. Y. Ueta, G. Springholz, G. Schinagl, G. Marschner, and G. Bauer, Thin Solid Films **306**, 320 (1997).
[17] G. Springholz, A. Y. Ueta, N. Frank, and G. Bauer, Appl. Phys. Lett. **69**, 2822 (1996).
[18] H. Krenn, W. Herbst, H. Pascher, Y. Ueta, G. Springholz, and G. Bauer (unpublished).
[19] J. Singleton, E. Kress-Rogers, A. V. Lewis, R. J. Nicholas, E. J. Fantner, G. Bauer, and A. Lopez-Otero, J. Phys. C **19**, 77 (1986).
[20] G. Grabecki, J. Wróbel, T. Dietl, M. Sawicki, J. Domagała, T. Skośkiewicz, E. Papis, E. Kamińska, A. Piotrowska, M. Leszczyński, Y. Ueta, G. Springholtz, and G. Bauer, Superlattices Microstruct. **22**, 51 (1997).
[21] E. Skuras, R. Kumar, R. L. Williams, J. E. Dmochowski, E. A. Johnson, A. Mackinnon, J. J. Harris, R. B. Beall, C. Skierbeszewski, J. Singleton, P. J. van der Wel, and P. Wisniewski, Semicond. Sci. Technol. **6**, 535 (1991).
[22] B. K. Ridley, *Quantum Processes in Semiconductors*, 3rd ed. (Oxford University Press, Oxford, 1993).
[23] S. Yuan, H. Krenn, G. Springholz, and G. Bauer, Phys. Rev. B **47**, 7213 (1993).
[24] G. Springholz, G. Ihninger, G. Bauer, M. M. Olver, J. Z. Pastalan, S. Romaine, and B. B. Goldberg, Appl. Phys. Lett. **63**, 2908 (1993).
[25] S. Yuan, G. Springholz, G. Bauer, and M. Kriechbaum, Phys. Rev. B **49**, 5476 (1994).
[26] See, e.g., H. Krenn, K. Kaltenegger, T. Dietl, J. Spałek, and G. Bauer, Phys. Rev. B **39**, 10 918 (1989).
[27] G. Bauer, H. Pascher, and W. Zawadzki, Semicond. Sci. Technol. **7**, 703 (1992).
[28] B. L. Altshuler and A. G. Aronov, Solid State Commun. **30**, 115 (1979).
[29] J. I. Ravich and W. I. Tamarchenko, Fiz. Tverd. Tela (Leningrad) **14**, 1945 (1972) [Sov. Phys. Solid State **14**, 2247 (1972)].
[30] A. Schmid, Z. Phys. **271**, 251 (1974).
[31] See, e.g., B. L. Altshuler, M. E. Gershenson, and I. L. Aleiner, Physica E **3**, 58 (1998).
[32] A. Mittal, R. G. Wheeler, M. W. Keller, D. E. Prober, R. E. Sacks, Surf. Sci. **361/362**, 537 (1996).
[33] P. Santhanam, S. Wind, and D. E. Prober, Phys. Rev. B **35**, 3188 (1987).
[34] W. E. Lawrence and A. B. Meador, Phys. Rev. B **18**, 1154 (1978).
[35] D. J. Thouless, Phys. Rep. **67**, 5 (1980); Solid State Commun. **34**, 683 (1980).
[36] J. Rammer and A. Schmid, Phys. Rev. B **34**, 1352 (1986).
[37] M. Y. Reizer and A. V. Sergeyev, Zh. Eksp. Teor. Fiz. **90**, 1056 (1986) [Sov. Phys. JETP **63**, 616 (1986)].
[38] H. Takayama, Z. Phys. **263**, 329 (1973).
[39] Yu. Kagan and A. P. Zhernov, Zh. Éksp. Teor. Fiz. **50**, 1107 (1966) [Sov. Phys. JETP **23**, 737 (1966)].
[40] D. Belitz and S. Das Sarma, Phys. Rev. B **36**, 7701 (1987).